Chapter 7 : Development of a model to simulate the spread of ascochyta blight of chickpea in the field

---

Manuscript prepared for submission to the journal *Plant Pathology*, except for coloured pictures, which will be adjusted to black and white for publication.

Development of a model to simulate the spread of ascochyta blight of chickpea in the field

S.A. Coventry[a,b] , M. U. Salam[c], J.A. Davidson[ad] and E.S. Scott[ab]

[a]Cooperative Research Centre for National Plant Biosecurity, LPO Box 5012, Bruce, ACT 2617, Australia; [b]School of Agriculture, Food and Wine, The University of Adelaide, PMB1, Glen Osmond, SA 5064, Australia; [c]Department of Agriculture and Food Western Australia, Locked Bag 4, Bentley Delivery Centre, Perth, WA 6983, Australia; [d]South Australian Research and Development Institute, GPO Box 397, Adelaide, SA 5001, Australia.

Abstract

Ascochyta blight, caused by *Didymella rabiei*, is a significant disease world-wide including southern Australia. To explore its intensity and pattern of spread, a weather-based spatio-temporal model was developed. The model, spread of *Ascochyta rabiei* in chickpea (SArC), is adapted from the previously published model, AnthracnoseTracer for lupins. The major parameters of the model were either derived from laboratory or field experimental data, or estimated through calibration with one year's field data. The model was then subjected to qualitative and quantitative validation using the following year's

field data; these data were not used for identifying parameters of the model. For quantitative validation, the performance of the model was analysed statistically using a confidence interval, correlation-regression approach and a deviation-based approach, and the model largely simulated the spread of the disease in fields in two chickpea cultivars of different resistance to ascochyta. Sensitivity analysis was then performed to show the relative sensitivity of the final model parameters. Given the strength of SArC model in the parameter estimation and calibration and validation, it has potential to be used as a tool in plant biosecurity and/or managing ascochtya blight in chickpea in farming systems.

Introduction

Ascochyta blight, caused by *Didymella rabiei*, is a significant disease in most of the world's chickpea (*Cicer arietinum L.*) crops and is a major constraint to chickpea production in Australia (Pande *et al.*, 2005). *D. rabiei* survives on infected seed and stubble, forming ascospores and/or conidia that initiate primary infection; ascospores are spread by wind and conidia by rain splash or wind-driven rain. Pycnidia develop on infected tissue, resulting in secondary spread through conidia that are dispersed by rain splash (Kaiser, 1997, Trapero-Casas & Kaiser, 1992b). In Australia, initiation and subsequent spread of this disease are attributed almost entirely to conidial infection and only one mating type (MAT 1-2) has been found to date (Phan *et al.*, 2003, Leo *et al.*, 2011). Dispersal of conidia occurs in wet and windy conditions (Shtienberg *et al.*, 2006, Kimber *et al.*, 2007); favourable conditions such as temperatures of 5-30 ºC optimum 20 ºC and relative humidity of > 95% are also required for the fungus to penetrate into and infect host tissues resulting in disease (Pande *et al.*, 2005, Jhorar *et al.*, 1997, Trapero-Casas & Kaiser, 1992a, Trapero-Casas & Kaiser, 2007).

Understanding the epidemiology of ascochyta blight with respect to interaction with host (e.g. degree of cultivar resistance) and environment (e.g. location-specific weather conditions) can help in formulating strategic and, to some extent, tactical management of the disease at a crop production level. It is impractical, given the limitations of resources and time, to investigate the epidemiology of a disease for each and every aspect of the host in all its growing environments. Thus, quantitative epidemiology from limited environments built into a model can aid in understanding epidemics in environments beyond its 'domain of study' (Salam *et al.*, 2011).

Empirical models, which provide a fit to observed data but do not necessarily take into account all the biological processes that explain the relationship, have been applied in epidemiology of plant pathogens since the 1960s (Van der Plank, 1964, Madden *et al.*, 2007). These models are valuable for determining a relationship between two or more variables and comparing the effects of treatments on biological processes (Madden *et al.*, 2007, Payne *et al.*, 2008). Logistic regression models are empirical models that have been used to describe the spatio-temporal development of *A. rabiei* on chickpea (Kimber *et al.*, 2007) and *Mycosphaerella pinodes* on field pea (Kimber *et al.*, 2007, Zhang *et al.*, 2004). Shtienberg *et al.* (2005) also used empirical modelling to identify the influence of temperature and wetness period on pseudothecial maturity of *Didymella rabiei* on chickpea debris, to identify the timing of chemical application most likely to prevent primary infection by ascospores. Such statistical models characteristically produce outputs without reference to underlying physical or biological variables, hence they are sometimes known as "black box" or "input-output" models. Also, extrapolation often is not possible using these statistical modelling techniques (Jones *et al.*, 2010). The other

broad class of models is known as mechanistic or simulation, as they explain causality between the variables by mimicking the system under consideration (Jones *et al*. 2010). Theories which identify key host and environmental interactions that influence the pathogen are devised at the beginning of development of these models, followed by mathematical representations, then validation, resulting in a working simulation model (Madden *et al.*, 2007). Simulation models are generally dynamic, meaning that they predict changes in epidemics over time (Jeger, 1986) and are of interest to plant pathologists undertaking disease predictions.

Many successful simulation models of plant diseases use weather as the driver to enable predictions for varying environmental conditions. Salam *et al.* (2003, 2011) have produced such models for predicting risk of diseases in Australian conditions. The models can predict the onset of pseudothecial maturity and seasonal showers of ascospores of phoma stem rot (blackleg) of oilseed rape (canola, *Brassica napus*) caused by *Leptosphaeria maculans* (Salam *et al.*, 2003) and severity and yield loss following release of ascospore of *Didymella pinodes,* cause of ascochyta blight (blackspot) of field peas (*Pisium sativum*) (Salam *et al.*, 2011). The risk of disease based on the models is made available every year to stakeholders. However, to the best of our knowledge, a model that can simulate the spread of *Ascochyta rabiei* on chickpea in the field has not been developed in Australia or elsewhere.

Diggle *et al.* (2002) developed a simulation model ("AnthracnoseTracer") for short distance rain-splashed dispersal of anthracnose of lupins, caused by *Colletotrichum gloeosporioides,* from infected seeds, the key epidemiology processes of which are similar to ascochyta blight of chickpea. In this study, we have adapted

"AnthracnoseTracer" to develop a spatio-temporal model for chickpea that simulates the spread of ascochyta blight at a field scale. The aims of this paper are to (i) describe the model, (ii) test the model with observed disease incidence in two chickpea cultivars of different ascochyta resistance, and (iii) perform sensitivity analyses.

Material and methods

The model, parameters, and estimation and/or calibration of parameters

The model, **S**pread of ***A**scochyta **r**abiei* on **C**hickpea (SArC) has two broad components: (i) the initiation, growth and spread of the pathogen (*Ascochyta rabiei*) on the host (chickpea crop) and (ii) growth of the host associated with the state of the disease (having no other potential physiological constraints). The model operates in a production unit (e.g. a field) which is segregated into smaller units of 1 m^2 area, henceforth designated a "model-operation-unit". The relational diagram of the model is shown in Figure 1. The model was written in Mathematica™ (Version 5.2, Wolfram Research Inc.).

SArC is driven by hourly weather variables, air temperature (º C), rainfall (mm), wind speed (m s^{-1}), wind direction (º), standard deviation of the wind direction (º) and the resistance of a chickpea cultivar to ascochyta blight (Table 1). Seedling density per model-operation-unit and initial infection point(s) in one or more model-operation-units are the initialisation variables of the model (Figure 1). The initial seedling density (SeedRate, an initialisation parameter) in a model-operation-unit is defined by the seeding rate of chickpea. A standard seeding rate of 45 seeds per m^2 was used as the value of this parameter (Day *et al.*, 2006). It was assumed that 40 of these 45 sown seeds would germinate and each seedling would have one growing point initially. In the "AnthracnoseTracer" model, infected seeds are the source of disease initiation; an

infected seed produces an infected growing point at seedling emergence. Infested pieces of stubble replaced infected seeds in SArC. The location of an infected growing point is represented in the model as the row-column co-ordinate of the model-operation-unit in the field. A field is assumed to be facing north as in the conventional cartographical orientation and a column number is designated from south to north and a row number from east to west. An infected growing point is a simplified representation of a lesion, and sporulates after completion of a latent period (LP), a parameter of the model. The latent period is the time between infection and production of sporulating lesions.

The latent period was calculated from laboratory and field observations. A single *A. rabiei* isolate (7706c) was cultured from storage and a suspension of 6×10^5 spores per ml prepared as described by Kimber *et al.* (2006). Plants of chickpea cultivars Howzat and Almaz were artificially spray inoculated until dripping and plants then placed in a chamber maintained at approximately 100 % relative humidity (RH). The temperature was maintained at approximately 18-20°C. Plants were monitored daily until pycnidia containing conidia were first observed, 9 days (180 degree-days) later for cv. Howzat (moderately susceptible) and 13 (260 degree-days) for cv. Almaz (moderately resistant). In the field, the latent period, from the time of inoculation with infested stubble to observation of pycnidia containing conidia on infected seedlings, was approximately 13 days for both cvs which was translated into approximately 150 degree days using onsite weather data from the Bureau of Meteorology (BOM). Galloway and MacLeod (2002) reported the latent period of *A. rabiei* on chickpea cvs Tyson (susceptible), Sona (susceptible) and Kaniva (highly susceptible) in controlled conditions at 20°C to be 8-9 days (160-180 degree days), RH not specified. Trapero-Casas and Kaiser (1992b) found a latent period of 5.5 days (100 degree days) on cv. Burpee (highly susceptible) at 20°C and

100 % RH. Accordingly, a latent period of 150 degree days was adopted for the SArC model.

The model assumes that each sporulating growing point produces a number of "potentially infective" spores. A potentially infective spore is defined as a spore that has the capability to cause infection on an uninfected growing point in suitable environmental conditions. The number of potentially infective spores produced per sporulating growing point (or sporulating lesion) is the parameter SporeRate of the model (Figure 1). Like the parent model, "AnthracnoseTracer", the SArC model does not consider in detail the dynamism of lesion formation. Furthermore, SporeRate is assumed to be constant, which implies that a sporulating growing point produces spores at a constant rate after formation. The SporeRate, an arbitrary number, differs between the chickpea cultivars depending on their level of resistance to ascochyta blight. In the parent model, this value was derived relative to that of a known lupin cultivar. In the SArC model, the value of SporeRate for two chickpea cultivars was derived through calibration. For this calibration, a set of values (0.15 to 0.60) with step 0.05 for cv. Howzat (Figure 2A) and for cv. Almaz (Figure 2B) parameter values of 0.050, 0.075, 0.08, 0.10 and 0.15 were chosen to encompass the potential range of sporulation rates. The model was run with each of the parameter values and the outputs were compared with observed field data (described below in validation of SArC model) through mean squared deviation (MSD) statistics (described below in MSD approach). The parameter value for each of the cultivars was finally estimated based on the closest agreement between the model outputs and observation (Figure 2 A and B).

The number of potentially infective spores spread from a model-operation-unit during a wet-hour is linearly related to the total number of sporulating growing points (SporuGP)

present in a given time. The model calculates the expected number of spores available for dispersion (NoSporeDisperse), in the given period, from a model-operation-unit as a random fractional value between 0-1, chosen from a Poisson distribution of the product of SporeRate and SporuGP.

Spread of *A. rabiei* spores, like that of other pathogens such as *Botrytis cinerea* or *Mycosphaerella pinodes* (Setti *et al.*, 2009, Saxena & Johansen, 1997, Taylor *et al.*, 2007), is initiated when favourable leaf wetness conditions are achieved. As leaf wetness data were not readily available, this is represented in the model in a simplified way by using a rainfall threshold of 0.1 mm in each hourly period (WHE) of model operation. In justifying using such a parameter value, in the parent model, Diggle *et al.* (2002) argued that 0.1 mm an hour or approximately 2 mm in a day would provide an adequate period of leaf wetness.

The spores expected to be dispersed are spread independently from each model-operation-unit that contains sporulating growing points (sporulating lesions). The model assumes that this dispersion originates from the centre of each model-operation-unit. The spores landing on the model-operation-unit may originate from the same model-operation-unit (m^2 quadrat) or from another model-operation-unit within or outside of the production unit (e.g. field). Dispersal of each potentially infective spore (DisperseSpore (angle, distance)) is a displacement vector with angle (θS) and distance (dS) components. This vector specifies the location at which the spore lands relative to its starting point. The actual dispersal is the vector sum of dispersal due to rain splash (DisperseSporeRain (angleRain,distanceRain)), and dispersal due to wind (DisperseSporeWind (angleWind,distanceWind)). The angle of dispersal due to rain splash (angleRain) is a

random number, with uniform probability from 0° to 360°. Wind-induced dispersal angle (angleWind) is chosen from a normal distribution defined by the average wind direction (°) in the hour and the standard deviation of wind direction as measured by a recording weather station. The distance component of dispersal due to rain splash (distanceRain in metres) is a random value chosen from a half-Cauchy distribution (Xu & Ridout, 1998) with median dispersal parameter RainDP:

$$\text{distanceRain} = \text{RainDP}\,(\pi\, z/2) \qquad \text{(Equation 1)}$$

where z is a uniform random number between 0 and 1. The RainDP is the median of the distribution distance in metres over which spores may travel. The distance component of dispersal (distanceWind) due to wind is calculated in the same way as distanceRain, but the median dispersal parameter, WindDP, is multiplied by the average wind speed (m s^{-1}) for the hour. Examples of distributions for the distance component of displacement due to a rain splash, and due to wind at measured wind speeds, are shown in Figure 3, which compares the model output with observations from wind tunnel experiments performed in 2007.

Dispersal of *A. rabiei* conidia from infested chickpea stubble was examined using a wind tunnel developed at the University of Adelaide (INSKIP Dust and Fume Extraction Pty Ltd). Spores were trapped on strips of clear high tack/medium tack double coated removable repositionable tape (3M™), 5 mm long x 2 mm wide, on 2 mm diameter metal rods. Tape was placed vertically at three positions on the rods (1-6, 11-16 and 31-35 cm). Rods were then placed at various distances along the 1.3 m long by 0.5 m wide observation chamber of the wind tunnel. Wind speeds were set at 1.4, 2.2, 3.3 and 4.7 m

s^{-1} and applied for 30 minutes at a time. When the experimental design required water, droplets were applied from 4 mm variable flow drippers inserted along an irrigation line inside the tunnel. Tape pieces were peeled from the rods at the end of an experimental run using fine tweezers and the number of conidia per tape counted microscopically. The counts of conidia at the various distances were thus used to estimate the parameter "spore deposition probability".

The probability that *A. rabiei* conidia will land on a given cm^2 after distribution by wind and rain is shown in Figure 3. The probability of conidia landing on a cm^2 area was high close to the source and greater wind speed increased the probability that conidia would land further from the source. Measured values taken at a wind speed of 1.4 m s^{-1} indicated that the probability of landing per cm^2 area was highest over 0.35 m from the source, with a probability of 0.007 cm^2, and declined to close to zero at 0.60 m. At 4.7 m s^{-1}, the measured probability of impact per cm^2 at 0.35 m was 0.010 and close to zero at 0.60 m. The model prediction for 1.4 m s^{-1} showed the probability of impact to be highest closer to 0.25 m with a probability of 0.020 cm^2. This became nearly zero at 0.60 m. The prediction of the impact for 4.7 m s^{-1} was 0.020 cm^2 at 0.40 m, but did not reach zero, indicating there is always a chance that a conidium will travel over 1.5 m.

It is unlikely that all potentially infective spores will produce infections because the density of receiving growing points in the target model-operation-unit is generally less than the total area of the model-operation-unit. In the model, the spore deposition probability (ProbableSporeDepo) is used to estimate successful infections from the number of potentially infective spores. The ProbableSporeDepo is calculated using an

exponential function similar to that commonly used for estimating the fraction of the incoming radiation intercepted by a crop canopy (Salam *et al.*, 1994).

ProbableSporeDepo = 1 – exp (-ProbableSporeLimit*UninfectedGP* InfectibilityMultiplier) (Equation 2)

ProbableSporeDepo is the limit of the probability of deposition of potentially infective spores in units of susceptible growing point per m^2 as the density of uninfected growing points (UninfectedGP InfectibilityMultiplier) approaches 0. The density of susceptible growing points on a square metre surface area is better expressed as susceptible growing point index, similar to leaf area index (LAI). In this study this was approximated by multiplying the uninfected growing points (UninfectedGP) by a multiplier (InfectibilityMultiplier) so that it simulated the pattern of LAI of the crop throughout the growing season. This multiplier (InfectibilityMultiplier) was approximated as 5, which closely matched the pattern of simulated LAI from APSIM (Agricultural Production Systems Simulator) model (module chickpea) runs for Roseworthy, South Australia, 2007 (courtesy of Dr. Imma Farre, Department of Agriculture and Food, Western Australia) (Figure 1 A, Appendix E). The number of susceptible growing points on each day is approximated as the product of InfectibilityMultiplier and the number of growing points formed on that day.

The growth of the chickpea plant is described by the development of growing points within each model-operation-section. Each seed sown, when germinated, produces one growing point which multiplies at a rate that is a function of temperature (GPREPrate)

and is limited by proximity to a maximum growing point density (GPmax). The number of new growing points (NewGP) in an iteration period of one day, is calculated as:

(NewGP = GPuninfected X GPREPrate X Temp (1 – GPuninfected / GPmax) (Equation 3)

where GPuninfected is the total number of uninfected growing points at the time of iteration, and Temp is the average daily temperature in °C. The parameter GPREPrate is defined as the rate of increase of the number of growing points per degree-Celsius per day (Figure 4 A and B).

Ten plants each of cultivars Howzat (MS) and Almaz (MR) were randomly selected at weekly intervals and the growing points (the number of main stems and the terminal and lateral shoots that developed from the main stems) were counted. Growing points were counted weekly from the start of the growing season, 12 June 2007, until the end of the growing season, 2 November 2007. This gave the estimation of the GPREPrat**e** and GPmax for each cultivar.

The number of growing points over time increased in a sigmoid curve for both cvs (Figure 4). Growing points on cv. Howzat (Figure 4 A) increased at a steady rate until a maximum of 5000 growing points m^2 at 1500 degree days. The correlation between observed values and the model prediction was $R^2 = 0.97$. Growing point density of cv. Almaz (Figure 4 B) increased exponentially to 1500 growing points m^2 at less than 750 degree days, and reached a maximum of almost 6000 growing points m^2 at 1500 growing

degree days. The observed values and the model prediction were closely correlated (R^2 = 0.92).

The model produced an output of the proportion of infected plants in a model-operation-unit, where N is the seedling density at sowing and SporuGP is the number of sporulating growing points, as follows:

Infected plants per model-operation-unit = $N - N(1-1/N)^{SporuGP}$ infective growing points per model-operation-unit (Equation 4)

Field data for model calibration and validation, and weather data for model operation

The spread of ascochyta blight on cvs Howzat, Almaz and Genesis 090 (Resistant) was studied in the field at Kingsford Research Station (S 34.55, E 138.78), South Australia in 2007 and Turretfield Research Station (S 34.55, E 138.82), South Australia in 2008. The trial in 2007 was termed the calibration plot as information was gathered from this plot to be used in calibration of the model. The trial in 2008 was termed a validation plot as it was only used to validate the model. Stubble with prominent lesions was used as a single source of inoculum placed centrally in each plot in 2007 and 2008. Plots were sown to dimensions 12 x 12 m in 2007 and in 2008, 11 m x 9.5 m, with a gap of 1.75 m between plots.

Plots were observed for disease expression at weekly intervals after placement of inoculum. Disease incidence was assessed each week starting in August, when disease was first observed, until the end of the growing season in November.

In 2007 and 2008, at the newly emerged seedling stage, each plot was subdivided into 1 m^2 observation quadrats, each of which contained 40 plants. Each plot was assigned a number, such that quadrat 1.1 was the focus and quadrat number increased in a clockwise direction away from the focus to the south of the plot, as shown in Figure 5. Each plot was assessed in a structured way, beginning at the perimeter (outermost, least infected middle quadrat, designated 5.1) and moving in a clockwise direction to the centre of the plot (most infected centre quadrat, 1.1) which contained the disease focus. Boots were sprayed with 70% ethanol before moving from one quadrat to the next. This sampling method was designed to reduce the potential for mechanical spread of the pathogen. An incidence score (0-100 %) was given as the percentage of the plants diseased of the total of 40 plants per m^2 quadrat.

The 2007 field data were used to calibrate the model and the 2008 data was used for model validation. To give uniform analysis the 11 x 9.5 m plot sown in 2008 was analysed over 9 x 9 m. The cultivar Genesis 090 was not modelled as no disease was observed.

Meteorological data were recorded at hourly intervals by an automated weather observation system (AWOS) (Telvent Australia Pty Ltd) at Roseworthy Research Station (S 34.51, E 138.68) situated 10 and 13 km from the site in 2007 and 2008, respectively. The data were accessed from the Climate & Consultative Services, Bureau of Meteorology (BOM), Adelaide, SA and downloaded via the Internet. The data collected comprised date and time, air temperature (°C), percentage relative humidity (% RH), average wind direction (°), standard deviation of wind direction (°), wind speed (m s^{-1}) and rainfall (mm).

Model validation and statistical analysis employed

The percentage of plants infected, the main output of the model, was subjected to qualitative and quantitative validation. In qualitative validation, observation and prediction for each m^2 unit were recorded on the lay-out of the plot; then each unit (m^2) was coloured according to five arbitrary categories: Low (0-30% of diseased plants, green); Medium (31-60%, yellow); High (61-80%, purple); and, Very high (81-100%, red).

The quantitative validation was performed for the whole plot (Figure 6 A) and two sections of the plot, inner (orange) and outer (yellow) (Figure 6 B). For this validation, the performance of the model was analysed statistically using a confidence interval, correlation-regression approach (prediction *versus* observation) and a deviation approach (prediction *minus* observation). The confidence interval was calculated for each mean at 99.9% (Conover, 1998). The purpose of this analysis was to explore if the range of the true mean between an observation and the corresponding prediction overlapped at very high (99.9%) confidence level. Logistic regression-based statistics were employed, $y = 1/\{1 + [(1 – y0)/y0] \exp(–ct)\}$ (Madden *et al.*, 2007, Zhang *et al.*, 2004). The purpose of this analysis was to identify the differences, if any, between the observation and the model prediction, with the estimated values of the logslopes compared using two tailed t-tests at $P < 0.05$ (from the student t-distribution table, Freund (1984). This was performed for three dates, 5 September, 3 October and 2 November 2008, for cvs Howzat and Almaz in two scenarios comparing (i) the slopes of the observed and model prediction of the whole plot (Figure 6 A), and (ii) the outer and inner sections of the plot (Figure 6 B). Statistical software, Genstat edition 10.1 (VSNI international Ltd) was used for this analysis.

The deviation-based statistics that were employed were mean squared deviation (MSD) (Equations 5-8).

$$MSD = SB + SDSD + LCS$$ Equation 5

$$SB = (\frac{1}{n}\sum_{i=1}^{n}(x_i - y_i))^2$$ Equation 6

$$SDSD = (\sqrt{\frac{1}{n}\sum_{i=1}^{n}(x_i - \bar{x}) - \sqrt{\frac{1}{n}\sum_{i-1}^{n}(y_i - \bar{y})})^2$$ Equation 7

$$LCS = 2(\sqrt{\frac{1}{n}\sum_{i=1}^{n}(x_i - \bar{x})(\sqrt{\frac{1}{n}\sum_{i=1}^{n}(y_i - \bar{y})}(1 - r)$$ Equation 8

Where, x is the model output, y is the measurement, xi and yi are the simulated and measured values, respectively, for the i-th from n number of measurements $\bar{x}$ and $\bar{y}$ are the means of xi and yi (i = 1, 2...n), and r is the correlation coefficient between the simulation and measurement. MSD has three additive components: (i) squared bias (SB), the first term of the right side of Equation 2; (ii) squared difference between predicted and observed standard deviations (SDSD), the second term of the right side of Equation 2 and (iii) lack of positive correlation weighted by the standard deviations of prediction and observation (LCS), the third term of the right side of Equation 2. MSD measures the total deviation between predictions and observations. The lower the value of MSD, the closer the prediction is to the observation. SB indicates the mean agreement between the model and observation, whereas SDSD and LCS together show how closely the model predicts variability around the mean. There are two sources of this variability, the magnitude of

fluctuation among the n observations and the pattern of the fluctuation across n observations; SDSD and LCS quantify the model's ability to describe the former and latter variability, respectively. Like the logistic regression approach, this was performed for both cvs Howzat and Almaz in two scenarios, (i) comparing the slopes of the observed and model prediction of the whole plot (Figure 6 A), and (ii) the outer and inner sections of the plot (Figure 6 B).

Sensitivity analysis

The parameters considered for the sensitivity analysis in the SArC model are presented in Table 2. These parameters explained development and dispersal of *A. rabiei* on chickpeas and were tested with values below and above the parameter set used in the model. A value 50% below and above of the model parameter set was applied for all but the latent period. The latent period was adjusted to a set value of 50 degree-days above or below the original value because an increase or decrease of a value by 50 degree-days represented varying latent periods reported in literature (Galloway & MacLeod, 2002, Trapero-Casas & Kaiser, 1992a).

Results

Observation versus Simulation – a qualitative comparison

Figures 7 and 8 (A to C) show the observed development of ascochyta blight on chickpea cvs Howzat and Almaz, in a pictorial scale, on each m^2 unit in the field, on 5 September, 3 October and 2 November compared with prediction from SArC. In 2008 the model slightly overestimated disease incidence in cv. Howzat at the beginning of the season and underestimated it at the end of the season (Figure 7 A to C). The spread of disease was influenced by the prevailing winds, blowing towards the SE direction. In contrast, disease

on cv. Almaz at the beginning of the season was slightly underestimated by the model but by the end of the season was slightly overestimated (Figure 8 A to C). Again, disease was influenced by wind blowing mainly towards the SE direction. The distribution of disease was patchy on 3 October (Figure 8 B) and 2 November (Figure 8 C); however, the model did not show any such patchiness in the prediction (Figure 8 A to C).

Observation versus Simulation – a quantitative comparison using confidence interval and logistic regression analysis

For both the cultivars, confidence interval (CI) statistics presented in Figure 9 (A to C) reveal that the 99.9% CI for the means for observation and prediction for each of the dates (5 September, 3 October and 2 November 2008) overlap, indicating a lack of significant difference between the observation and the model prediction.

The slopes of the logistic regression for disease incidence across the whole plot showed no significant difference ($P > 0.05$) between observation and prediction (Table 3) for cvs Howzat and Almaz.

Table 4 shows the slopes of the logistic regression for disease incidence, across the inner and outer sections of the plot, for the observation and prediction in cvs Howzat and Almaz. The model prediction for the inner section differed significantly ($P < 0.05$) from the observation on 3 October 2008 and 2 November 2008 for cv. Howzat. The same was true for the outer early (5 September 2008) and late (2 November 2008) observations. For the cv. Almaz, slopes observations and predictions were similar for both the inner or outer sections.

Observation versus Simulation – a quantitative comparison using MSD approach

Across the whole validation plot, the difference between observation and prediction for the early measured data (5 September 2008) is evident in Figure 10 (A), which shows the MSD for cvs Howzat and Almaz to be 320 and 153, respectively. Both deviations were largely attributed to LCS i.e. variability, in terms of pattern of fluctuation around the mean. With the subsequent data (on 3 October 2008), deviation between prediction and observation for both cultivars was also largely attributed to LCS. At the final assessment (2 November 2008), the MSD between observation and model prediction was attributed mainly to LCS for cv. Almaz, but to SDSD for cv. Howzat.

In the inner section of the validation plot (Figure 10B), the MSD analysis indicates that differences between observation and prediction for cv. Howzat were due predominantly to LCS. However, the squared bias (SB) also contributed to this deviation in the early observation (5 September 2008) (Figure 10B). In cv. Almaz, the MSD analysis indicates that, for all three observation dates, the difference between observation and prediction was mainly due to LCS; however, in the later two measurements (3 October and 2 November 2008) SB also contributed to MSD.

While the overestimation of plant infection in the outer section of the validation plot when the model was run for both cultivars with data for 3 October 2008 was attributed to LCS, the SB also contributed to a significant proportion of the overall MSD in cv. Howzat (Figure 10 C). With the 02 November 2008 data, the deviation (MSD = 987 for Howzat and 1121 for Almaz) between observation and prediction was similar for both the cultivars (Figure 10 C). Here, the attribution of the deviations (MSD) was not similar for

the two cultivars; the MSD components SDSD and LCS played a leading role in causing the deviation in cv. Howzat and Almaz, respectively.

Sensitivity of parameter in SArC model

Figure 11 shows the sensitivity of six parameters of the SArC model in simulating the spread of *A. rabiei* in the field. With respect to relative change in model output in terms of percent plant infection, three parameters appeared to be less sensitive in that they caused variation in model output of about 10% or less. Of these parameters, two (DistanceWind, DistanceRain) related to dispersion of spores by wind and rain, and the other (LP) was latent period. The parameter that drives the model with respect to the probability of deposition of potentially infective spores on a chickpea plant (ProbableSporeDepo) was moderately sensitive to the increased but not the decreased values. The same was true for the parameter SporeRate that denotes the number of potentially infective spores produced per sporulating lesion. The GPREPRate, i.e. the growth of the chickpea plant as described by growing point development, was the most sensitive parameter of the model (Figure 11). An increased and reduced value of this parameter resulted in about 70 and 25% reduction in model output, respectively.

Discussion

The SArC model, developed in this study, is the first model simulating the spread of the pathogen *Ascochyta rabiei* and ascochyta blight on chickpeas in a natural environment. The principles and structure of the model are based on the published model "AnthracnoseTracer" (Diggle *et al.* 2002) and other literature (Xu & Ridout, 1998). AnthracnoseTracer, which simulates the spread of anthracnose in lupins, was largely theoretical, therefore, a main focus in developing the SArC model was to acquire

experimental data for estimation and calibration of parameters. The other focus was to validate the model with extensive field data. These aspects have greatly strengthened confidence in the model with respect to its operational and predictive values.

Eight of nine parameters of the model were either estimated or calibrated with laboratory or field experimental data. The exception was the rainfall threshold which was taken from published literature, which reflects the minimum amount of leaf wetness required for germination of spores and successful penetration of host tissue (Diggle *et al.* 2002).

Three-step model validation, using independent data on percent plant infection recorded three times in the field from each square metre quadrat of a 9 by 9 m plot, was encouraging. Independent data were not used for any processes of development of the SArC model. A pictorial representation, the first step of the model validation employed in this study, was intended to provide a general impression, or snapshot, of the model's capability of simulating the observation. A similar snapshot of model output was published previously for phoma stem canker of oilseed rape (Aubertot *et al.*, 2006). The present qualitative validation showed that the model, in general, capably predicted the observed spread of ascochyta blight in Howzat and Almaz, two cultivars of chickpea that differed in resistance. This inference is supported in the first part of the two-step model validation, where it was observed that the 99.9% confidence intervals for the mean values of the observations and the predictions overlapped, indicating that the values were likely to be similar (Madden *et al.*, 2007), The second part of the model validation, in which the statistical significance (t-statistics) of the slopes of logistic equations for the observation and prediction was tested, showed that the model agreed with observations for all comparisons on three dates of data recording for both the cultivars, when the average of

the data of the whole validation plot was used. This was also true for comparisons of the inner and outer sections of the validation plot for cv. Almaz, although there was some discrepancy between observation and model prediction for cv. Howzat. The small sample size with the many zeros present in the data, when the plot was analysed in two sections, is likely to have caused overestimation of the effect measure, indicated by the large regression slopes (Nemes *et al.*, 2009). This indicates that this analysis may not be reliable in estimating accurately the slope due to the zeros values present.

A difference or deviation between the model prediction and reality (or observation) is expected, as reality is always simplified in a model, partly because our understanding of basic processes is limited, partly because this enables us to handle the model (Salam, 1992). Furthermore, models in biological systems are working hypotheses and it is not possible to prove hypotheses absolutely in science (Whisler *et al.*, 1986). Thus, modelling is a continuous process aimed at improving predictability. To improve the accuracy of the model's prediction, a first step should be to identify the discrepancies between prediction and observation. The MSD analysis in the third step of model validation provided the opportunity to locate the major cause of deviation between model prediction and observation. In this study, LCS appeared to be the major deviation between observation and prediction. The LCS denotes the lack of positive correlation weighted by the standard deviations of the prediction and observation; it is one of the three additive components of MSD. Together with SDSD, the LCS shows how closely the model predicts variability around the mean. There are two sources of this variability, the magnitude of fluctuation among the n observations and the pattern of the fluctuation across n observations; the LCS quantifies the model's ability to simulate the latter variability. One of the reasons that the model could not simulate some of the observed

disease spread may be simplification of the infection process. Unusual patterns of disease spread were occasionally observed in the field. For example, severe disease occurred in the north-east section of the plot of cv. Almaz on 3 October and 2 November (Figure 8, B and C), which was not predicted by the model. The disease observed may have been due to mechanical spread or other phenomena such as gusts of wind. The model simulated less disease in the north-western corner of c.v Howzat (Figure 7, B and C) than was observed. Again, the model did not simulate this event, thus further tweaking of the model may lead to closer simulation of these occurrences.

The model is a simplified version of spread and infection caused by *A. rabiei* in the field and does not encompass every detail of the interaction. For example, it does not take into account the dynamics associated with turbulent winds, continuously changing wind directions and topography, which would add complexity to the model. Gust of winds create turbulence near the leaf surface and can disperse spores upwards to be caught in laminar winds (Sache, 2000); if spores are transported high enough via gusts they can reach the laminar boundary level where they can travel many kilometres (Lacey & West, 2006). The pattern of spore dispersal was studied in a wind and rain tunnel with laminar flow of air, thus further research is needed to estimate dispersal in turbulent winds to model this phenomenon. Moderately resistance cvs of chickpea have also been shown to decrease in resistance as the plants age (Basandrai *et al.*, 2007, Chongo & Gossen, 2001). Reduction of resistance as plants age may explain why the moderately resistant cv. Almaz showed unusual disease occurrence in the north-east section of the plot as the crop matured, thus resistance may need to be adjusted overtime within the model to increase accuracy.

In modelling, certainty in parameters is always an issue. Sensitivity analysis tests how responsive the model is to changes in certain parameters (Whisler *et al.*, 1986). When a parameter is insensitive or less sensitive, for example parameters related to rain and wind-assisted dispersal and latent period in the SArC model, this implies that it is robust, so improving this parameter value will contribute least to performance of the model; also when applying the model in different environments, calibration of this parameter could be a lesser priority. Sensitivity analysis showed the SArC model to be very sensitive to growing point replication rate (GPRepRate) and spore replication rate (SporeRate). The value of the growing point replication rate was calculated using field experiments; therefore, there is little scope to improve this parameter. However, this sensitivity provides a caution that special attention may be required to assign the value of the parameter when the model is applied to an environment different from that in which it was tested. The other sensitive parameter, the spore replication rate, was derived from model calibration. This reflects the degree of resistance to ascochyta blight. It is an important parameter and future research should aim to quantify the productivity of conidia.

Given the strength of the SArC model in the validation and the scope identified for its improvement, it has potential to be used as a tool in plant biosecurity and/or managing ascochtya blight in chickpea. For example, in the field of biosecurity, it may be used to predict the spread of exotic plants pathogens such as anthracnose on lentils (*Colletotrichum truncatum*), and to study the implications if the disease were to occur in Australia. From a disease management point of view, the model might be used to identify the scale of potential damage, if any. It can also be used to examine the effect of cv. on disease spread and could help farmers decide which cultivars to sow.

This study has produced the first simulation model to predict the spread of *Ascochyta rabiei*. Although some aspects of the model need further investigation to determine applicability in other agroecological regions outside of South Australia, the model will be useful for chickpea growers as an ascochyta management tool and, with further development, could be used to predict exotic plant pathogens with similar dispersal methods.

Acknowledgements

We thank the Crop Improvement Group, South Australian Research and Development Institute (SARDI) for chickpea seed and site maintenance. This project formed part of the PhD program of Mr Steven Coventry, with support from the Cooperative Research Centre for National Plant Biosecurity, SARDI, Department of Agriculture and Food Western Australia and the University of Adelaide.

References

Aubertot JN, West JS, Bousset-Vaslin L, Salam MU, Barbetti MJ, Diggle AJ, 2006. Modelling for integrated avirulence management: Case study of phoma stem canker of oilseed rape (*Brassica napus*). *European Journal of Plant Pathology* **114**, 91-106.

Basandrai AK, Basandrai D, Pande S, Sharma M, Thakur SK, Thakur HL, 2007. Development of ascochyta blight (*Ascochyta rabiei*) in chickpea as affected by host resistance and plant age. *European Journal of Plant Pathology* **119**, 77-86.

Chongo G, Gossen BD, 2001. Effect of plant age on resistance to *Ascochyta rabiei* in chickpea. *Canadian Journal of Plant Pathology* **23**, 358-63.

Conover WJ, 1998. *Practical Nonparametric Statistics*. New Jersey, USA: John Wiley & Sons, Inc.

Day T, Day H, Hawthorne W, Mayfield A, McMurray L, Rethus G, Turner C, 2006. Grain Legume Handbook. In: Lamb J, Poddar A, eds. Riverton, South Australia: Finsbury Press.

Diggle AJ, Salam MU, Thomas GJ, Yang HA, O'Connell M, Sweetingham MW, 2002. AnthracnoseTracer: A spatiotemporal model for simulating the spread of anthracnose in a lupin field. *Phytopathology* **92**, 1110-21.

Freund J.E, 1984. *Modern Elementary Statistics*. New Jersey, USA: Prentice-Hall.

Galloway J, MacLeod B, 2002. Epidemiology of ascochyta and botrytis disease of pulse. *Department of Agriculture Western Australia, Crop Updates*, 91-5.

Jeger MJ, 1986. The potential of analytic compared with simulation approaches to modeling in plant disease epidemiology. In: Leonard KJ, Fry WE, eds. *Plant disease epidemiology: population dynamics and management.* New York, USA: Macmillan Publishing Co., 255-81.

Jhorar OP, Mathauda SS, Singh G, Butler DR, Mavi HS, 1997. Relationships between climatic variables and Ascochyta blight of chickpea in Punjab, India. *Agricultural and Forest Meteorology* **87**, 171-7.

Jones RA, Salam MU, Maling T, Diggle AJ, Thackray DJ, 2010. Principles of predicting plant virus disease epidemics. *Annual Review of Phytopathology* **48**, 179-203.

Kaiser WJ, 1997. Inter and intranational spread of ascochyta pathogens of chickpea, faba bean, and lentil. *Canadian Journal of Plant Pathology* **19**, 215–24.

Kimber RBE, Scott ES, Ramsey MD, 2006. Factors influencing transmission of *Didymella rabiei* (Ascochyta blight) from inoculated seed of chickpea under controlled conditions. *European Journal of Plant Pathology* **114**, 175-84.

Kimber RBE, Shtienberg D, Ramsey MD, Scott ES, 2007. The role of seedling infection in epiphytotics of Ascochyta blight on chickpea. *European Journal of Plant Pathology* **117**, 141-52.

Lacey ME, West JS, 2006. *The Air Spora: A Manual for Catching and Identifying Airborne Biological Particles*. Dordrecht, the Netherlands: Springer.

Leo AE, Linde CC, Elliott V, Lindbeck K, Ford R, 2011. Population structure of *Ascochyta rabiei* in Australia, using the newly developed microsatellite loci markers. *Proceedings of the Australasian Conference for Plant Pathology, Australasian Plant Pathology Society*. Darwin, Australia, p 80.

Madden LV, Hughes G, Bosch F, 2007. *The Study of Plant Disease Epidemics*. Minnesota, USA: American Phytopathological Society Press.

Nemes S, Jonasson JM, Genell A, Steineck G, 2009. Bias in odds ratios by logistic regression modelling and sample size. *BMC Medical Research Methodology* **9**, 56.

Pande S, Siddique KHM, Kishore GK, Bayaa B, Gaur PM, Gowda CLL, Bretag TW, Crouch JH, 2005. Ascochyta blight of chickpea (*Cicer arietinum* L.): a review of biology, pathogenicity and disease management. *Australian Journal of Agricultural Research* **56**, 317-32.

Payne RW, Harding SA, Murray DA, Soutar DM, Baird DB, Glaser AI, Channing IC, Welham SJ, Gilmour AR, Thompson R, Webster R, 2008. *A guide to regression, nonlinear and general linear and general linear models in genstat*. VSN International, Hertfordshire, United Kingdom.

Phan HTT, Ford R, Taylor PWJ, 2003. Population structure of *Ascochyta rabiei* in Australia based on STMS fingerprints. *Fungal Diversity* **13**, 111-29.

Sache I, 2000. Short distance dispersal of wheat rust spores by wind and rain. *Agronomie* **20**, 757-67.

Salam MU, Khangura RK, Diggle AJ, Barbetti MJ, 2003. Blackleg Sporacle: A model for predicting onset of pseudothecia maturity and seasonal ascospore showers in relation to blackleg of canola. *Epidemiology* **93**, 1073-81.

Salam MU, 1992. *A systems approach to the potential production of Boro rice in the Haor region of Bangladesh*. United Kingdom: University of Reading, PhD Thesis.

Salam MU, Galloway J, Diggle AJ, MacLeod WJ, Maling T 2011. Predicting regional scale spread of ascospores of *Didymella pinodes* causing ascochyta blight disease on field pea. *Australasian Plant Pathology* On-line [http://www.springerlink.com/content/n72235012n8p2802/]

Salam MU, Street PR, Jones JGW, 1994. Potential production of Boro rice in the Haor region of Bangladesh: Part 1. The simulation model, validation and sensitivity analysis. *Agricultural Systems* **46**, 257-78.

Saxena NP, Johansen C, 1996. Integrated management of botrytis gray mold of chickpea: agronomic and physiological factors. *Proceedings of the Third Working Group Meeting on Botrytis Gray Mold of Chickpea, 1997*. Pantnagar, Uttar Pradesh, India, pp 21-8.

Setti B, Bencheikh M, Henni J, Neema C, 2009. Effect of pea cultivar, pathogen isolate, inoculum concentration and leaf wetness duration on Ascochyta blight caused by *Mycosphaerella pinodes*. *Phytopathologia Mediterranea* **47**, 214-22.

Shtienberg D, Gamliel-Atinsky E, Retig B, Brener S, Dinoor A, 2005. Significance of preventing primary infections by *Didymella rabiei* and development of a model to estimate the maturity of pseudothecia. *Plant Disease* **89**, 1027-34.

Shtienberg D, Kimber RBE, McMurray L, Davidson JA, 2006. Optimisation of the chemical control of Ascochyta blight in chickpea. *Australasian Plant Pathology* **35**, 715-24.

Taylor P, Lindbeck K, Chen W, Ford R, 2007. Lentil diseases. In: Yadav SS, Mcneil DL, Stevenson PC, eds. *In Lentil: An ancient crop for modern times* Dordrecht, the Netherlands: Springer Verlag, 291-313.

Trapero-Casas A, Kaiser WJ, 1992a. Development of *Didymella rabiei,* the teleomorph of *Ascochyta rabiei*, on chickpea straw. *Phytopathology* **82**, 1261-6.

Trapero-Casas A, Kaiser WJ, 1992b. Influence of temperature, wetness period, plant age, and inoculum concentration on infection and development of ascochyta blight of chickpea. *Phytopathology* **82**, 589-96.

Trapero-Casas A, Kaiser WJ, 2007. Differences between ascospores and conidia of *Didymella rabiei* in spore germination and infection of chickpea. *Phytopathology* **97**, 1600-7.

Van Der Plank JE, 1964. *Plant Diseases: Epidemics and Control*. New York and London: Academic Press Inc.

Whisler FD, Acock B, Baker DN, Fye RE, Hodges HF, Lambert JR, Lemmon HE, MkKinion JM, Reddy VR, 1986. Crop simulation models in agronomic systems. *Advances in Agronomy* **40**, 141-208.

Xu XM, Ridout M.S, 1998. Effects of initial epidemic conditions, sporulation rate, and spore dispersal gradient on the spatio-temporal dynamics of plant disease epidemics. *Phytopathology* **88**, 1000-12.

Zhang JX, Fernando WGD, Xue AG, 2004. Temporal and spatial dynamics of mycosphaerella blight (*Mycosphaerella pinodes*) in field pea. *Canadian Journal of Plant Pathology* **26**, 522-32.

Table 1 Cultivar description, seed source and ascochyta blight rating of chickpeas used in the field trials at Kingsford in 2007 and Turretfield in 2008.

Chickpea cultivar and description	Resistance rating [a]	Seed source [b]
Howzat - Desi type, medium to tall height, early flowering, medium size, light brown seed	MS	Balaklava, SA
	MS	Turretfield, SA
Almaz - Kabuli type, medium height, late flowering, large cream seed	MR	Riverton, SA
	MR	Turretfield, SA
Genesis 090 - Kabuli type, medium height, mid flowering, medium to small cream seeds	R	Riverton, SA
	R	Turretfield, SA

a. MS = moderately susceptible, MR = moderately resistant, R = resistant

b. Seeds were sourced from chickpea breeding trials and commercial trials in South Australia (SA)

Table 2 Parameter sensitivity, comprising the parameter description, the unit, the original model parameter values, and the adjusted range (± 50 % or ± 50). The latent period of 150 degree days was adjusted by ± 50 based on latent periods found in the literature and through experiment.

Biological parameter description	**Unit**	**Model parameter value**	**Tested range**	**Low**	**High**
Growth of the chickpea plant as described by growing point development	GPREPRate	0.0065	± 50 %	0.00325	0.00975
The probability of deposition of potentially infective spores on a chickpea plant	ProbableSporeDepo	0.000065	± 50 %	0.0000325	0.0000975
Distance a spore is transported by rain	DistanceRain	0.015	± 50 %	0.0075	0.0225
Distance a spore is transported by wind	DistanceWind	0.015	± 50 %	0.0075	0.0225
The number of potentially infective spores produced per sporulating lesion	SporeRate	0.220	± 50 %	0.11	0.33
The period of time between infection and production of sporulating lesions	LP	150	± 50	100	200

Table 3 Logistic regression analysis of the observed incidence of ascochyta blight across the whole plot compared to the model prediction of incidence on 5 September 2008, 3 October 2008 and 2 November 2008 for chickpea cultivars Howzat and Almaz. SE ± of the residual are shown for the logit data. The regression slopes were compared for the model and the observation. Significance was determined by student t-distribution table ($P < 0.05$) from 80 observations.

			Whole plot		
Cultivar	Date	Model	logSlope	SE ±	t-statistic
Howzat	5/09/2008	Observation	0.07	0.12	-0.23
		Prediction	0.10	0.09	
	3/10/2008	Observation	0.21	0.09	-0.39
		Prediction	0.52	-0.80	
	2/11/2008	Observation	0.00	18.32	-0.04
		Prediction	0.70	0.12	
Almaz	5/09/2008	Observation	0.08	0.10	-0.17
		Prediction	0.10	0.11	
	3/10/2008	Observation	0.13	0.10	-0.59
		Prediction	0.21	0.08	
	2/11/2008	Observation	0.17	0.11	-0.56
		Prediction	0.24	0.08	
	*** indicates significant at P < 0.05**				

Table 4 Logistic regression analysis of the observed incidence of ascochyta blight across the inner and outer sections of the plot compared to the model prediction of incidence on 5 September 2008, 3 October 2008 and 2 November 2008 for chickpea cultivars Howzat and Almaz. The regression slopes were compared for the model and the observation. SE ± of the residuals are shown for the logit data. Significance was determined by student t-distribution table ($P < 0.05$) from 24 observations for the inner and 45 observations for the outer sections.

			logSlope		SE ±		t-statistic	
Cultivar	Date	Model	Outer	Inner	Outer	Inner	Outer	Inner
Howzat	5/09/2008	Observation	0	0.06	0.01	0.07	-3.65*	-0.62
		Prediction	0.09	0.11	0.02	0.05		
	3/10/2008	Observation	0.11	0.08	0.03	0.06	1.27	-4.28*
		Prediction	0.07	1.64	0.02	0.36		
	2/11/2008	Observation	0	0	0.01	0.02	-3.69*	-159.45*
		Prediction	0.09	5.50	0.02	0.02		
Almaz	5/09/2008	Observation	0	0.08	0.01	0.05	-0.52	0.54
		Prediction	0.01	0.04	0.03	0.06		
	3/10/2008	Observation	0.62	0.18	0.70	0.06	0.80	1.40
		Prediction	0.05	0.08	0.02	0.05		
	2/11/2008	Observation	0.15	0.23	0.05	0.08	1.78	1.10
		Prediction	0.06	0.13	0.02	0.06		
	*** indicates significant at P < 0.05**							

Figure 1 Relational diagram of the SARC (spread of *Ascochyta rabiei* on chickpea) model including the development and dissemination of *A. rabiei* in a chickpea field represented by the model. Ovals (blue) represent the parameters of the model identified through calibration or investigation; Bold (orange) ovals represent initialisation variables used to run the model; ovals (yellow) represent information used to drive the simulation process.

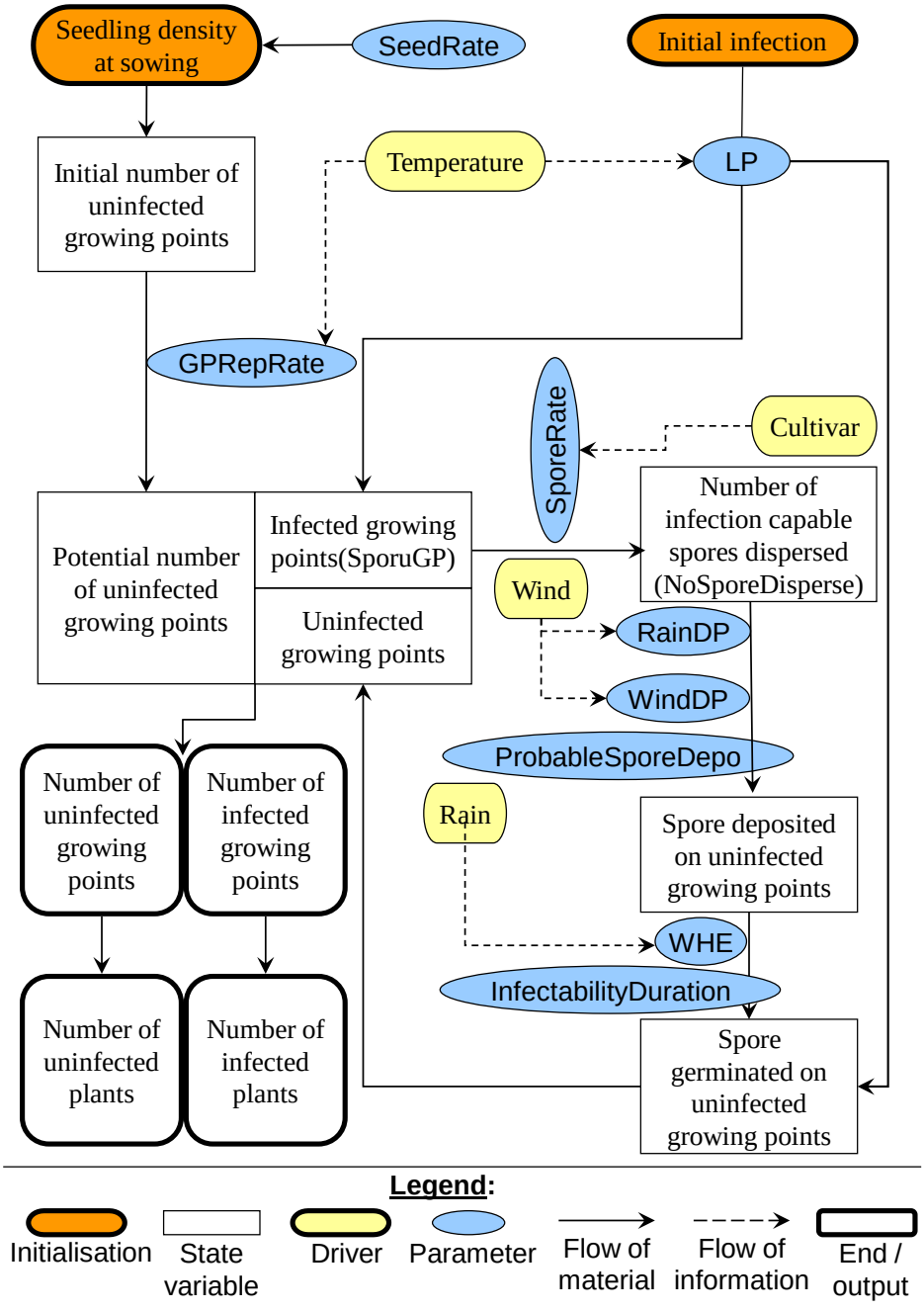

Figure 2 Calibration of the parameter SporeRate for chickpea cultivars Howzat (A) and Almaz (B) for 15 September, 12 October and 2 November 2007. Values of 0.15 to 0.60, with a step of 0.05, were used in calibrating cv. Howzat. Values of 0.050, 0.075, 0.08, 0.10 and 0.15 were used in calibrating cv. Almaz. The parameters which showed closest agreement between model output and observations for each cultivar were applied to the model as the SporeRate parameter. SporeRate is assumed to be constant so that a sporulating growing point produces spores at a constant rate after formation. The SporeRate is an arbitrary number.

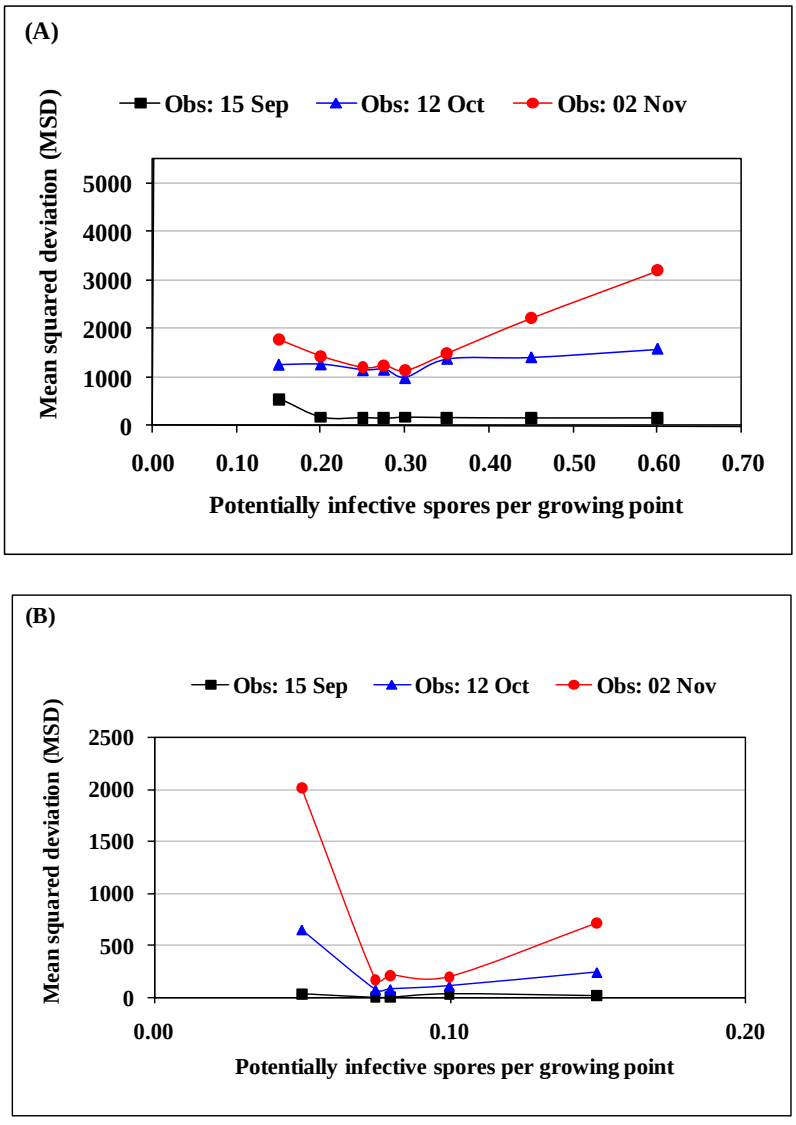

Figure 3 The measured and predicted probability that conidia of *A. rabiei* will land on a given cm^2 area in the presence of rain plus wind at 1.4 to 4.7 m s^{-1}. Measured data were obtained from wind and rain tunnel experiments and the prediction was calculated via the equation, distanceRain = RainDP (π z/2), where z a uniform random number on the interval between 0 and 1.

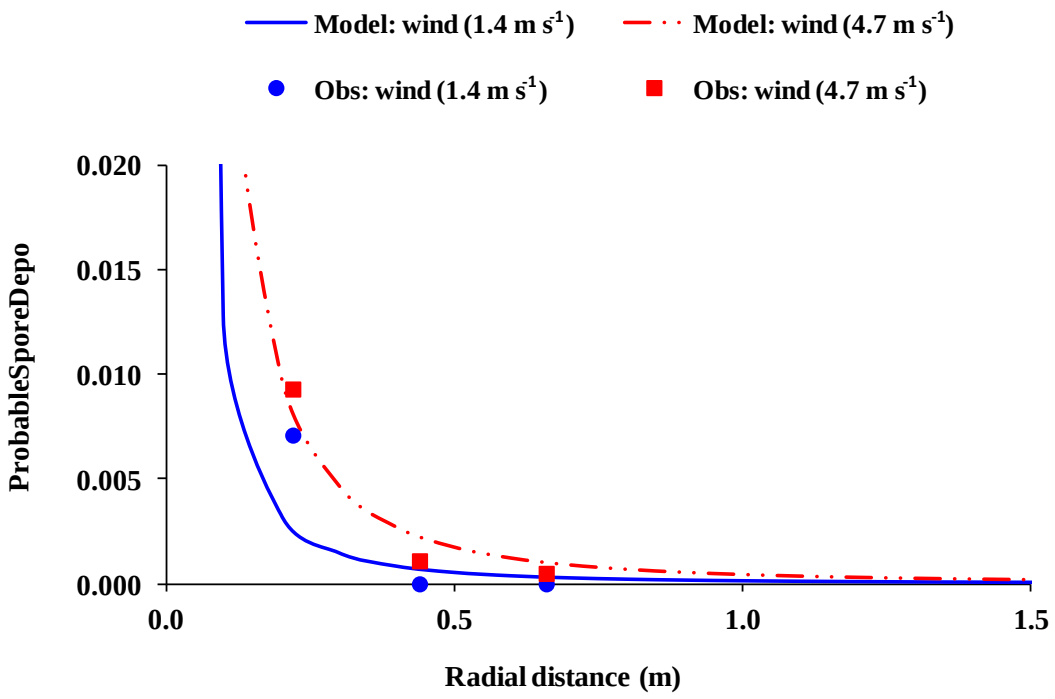

Figure 4 (A) and (B) The growing point density of chickpea cvs Howzat (A) and Almaz (B) per m^2. Growing point development was recorded at Kingsford, South Australia in 2007. Growing points (main stem development and lateral shoot development) were calculated using growing degree-days (number accumulated degree-days above the base temperature taken from first infection observation). The line (-) indicates the model prediction and the symbol (•) indicates the measured values of growing points.

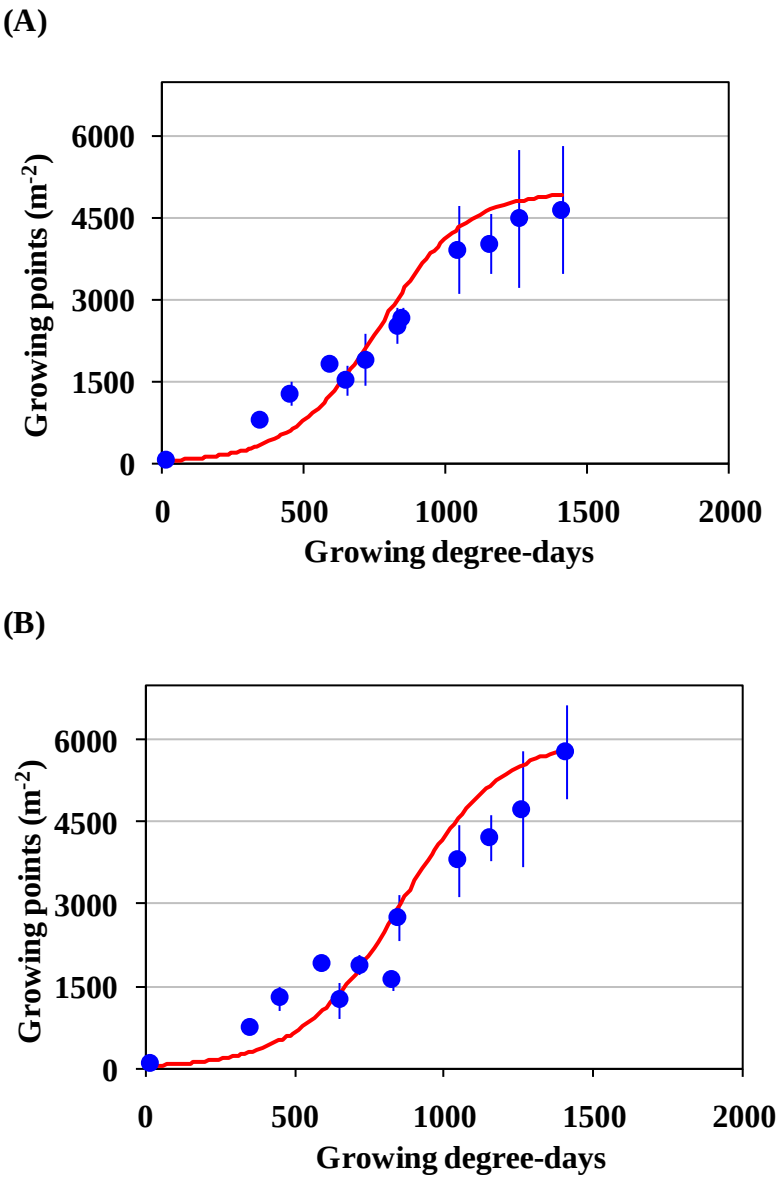

Figure 5 Disease assessment strategy for each cultivar in field trials. Quadrats, 1 m^2, were assigned numbers as follows: 1.1 for the centre quadrat; 2.1 to 2.8, in a clockwise direction for the next quadrats; 3.1 to 3.16 in a clockwise direction for the next quadrats; 4.1 to 4.24 in a clockwise direction for the next quadrats; 5.1 to 5.32 in a clockwise direction for the next quadrats. Dashed arrows from 5.1 to 1.1 and back to 5.1 indicate entry and exit points used when assessing disease. Solid arrows show the pattern in which disease was assessed, proceeding in a clockwise direction.

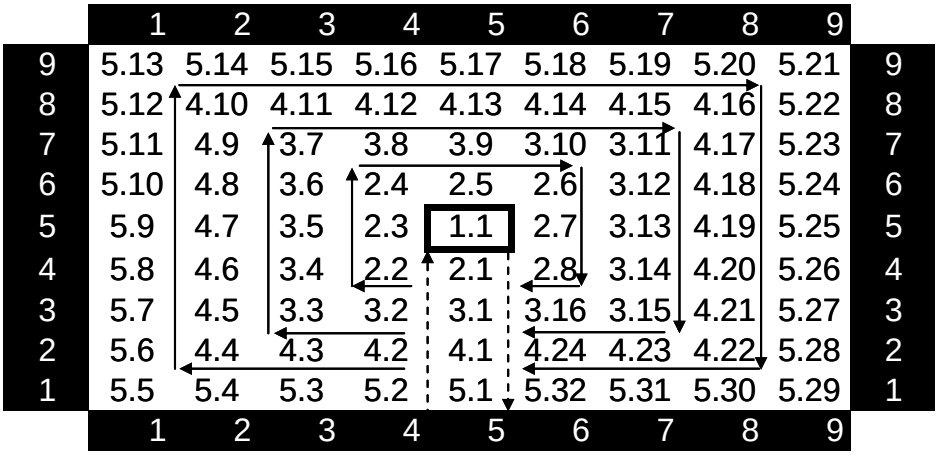

Figure 6 (A) Statistical design for the 9 x 9 m plot to compare the accuracy of the observed and the model prediction output for cvs Howzat and Almaz on the whole plot level (dotted shading) and **(B)** over two sections of the plot, the inner (dotted) and outer (checked shading) of the plot.

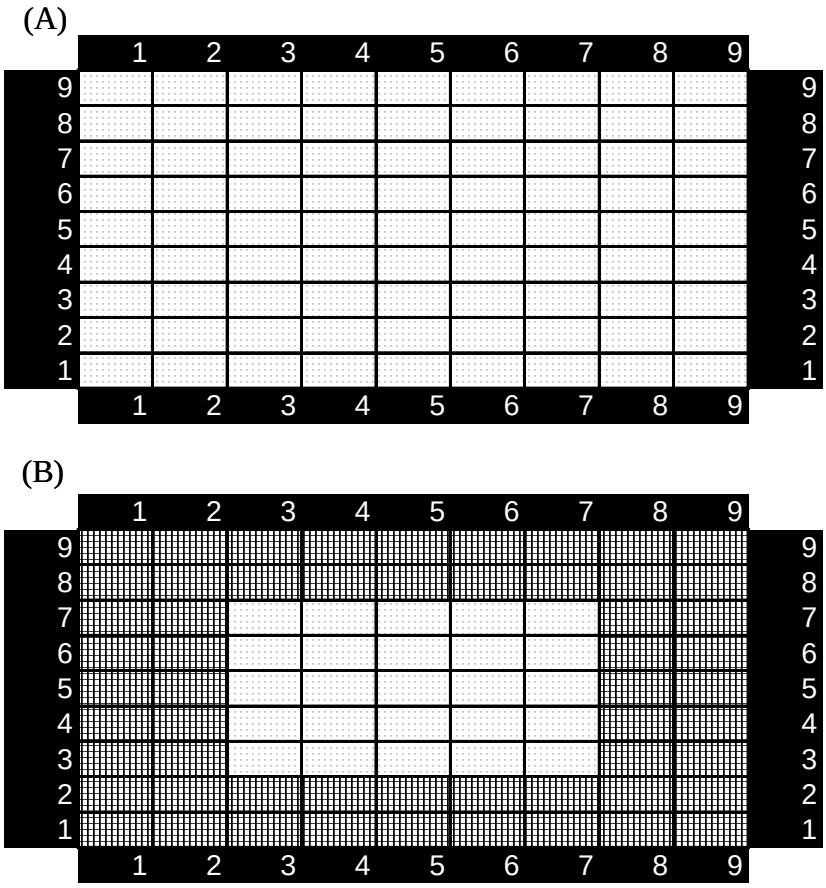

Figure 7 The percentage of plants infected per m^2 in a 9 x 9 plot planted with cv. Howzat. Observation and prediction on (A) 5 September 2008, (B) 3 October 2008 and (C) 2 November 2008.

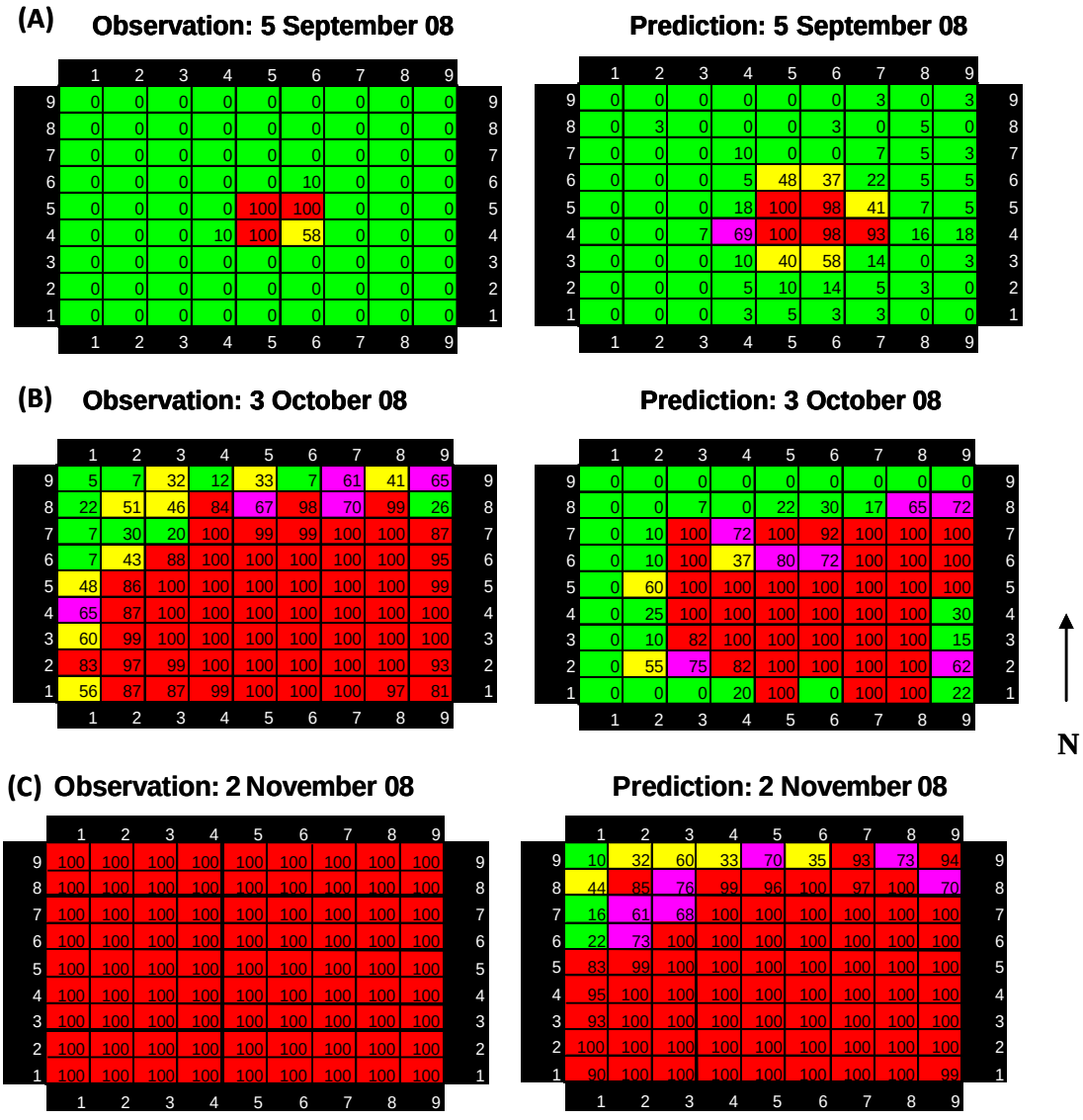

Figure 8 The percentage of plants infected per m^2 in a 9 x 9 m plot planted with cv. Almaz. Observation and prediction on (A) 5 September 2008, (B) 3 October 2008 and (C) 2 November 2008.

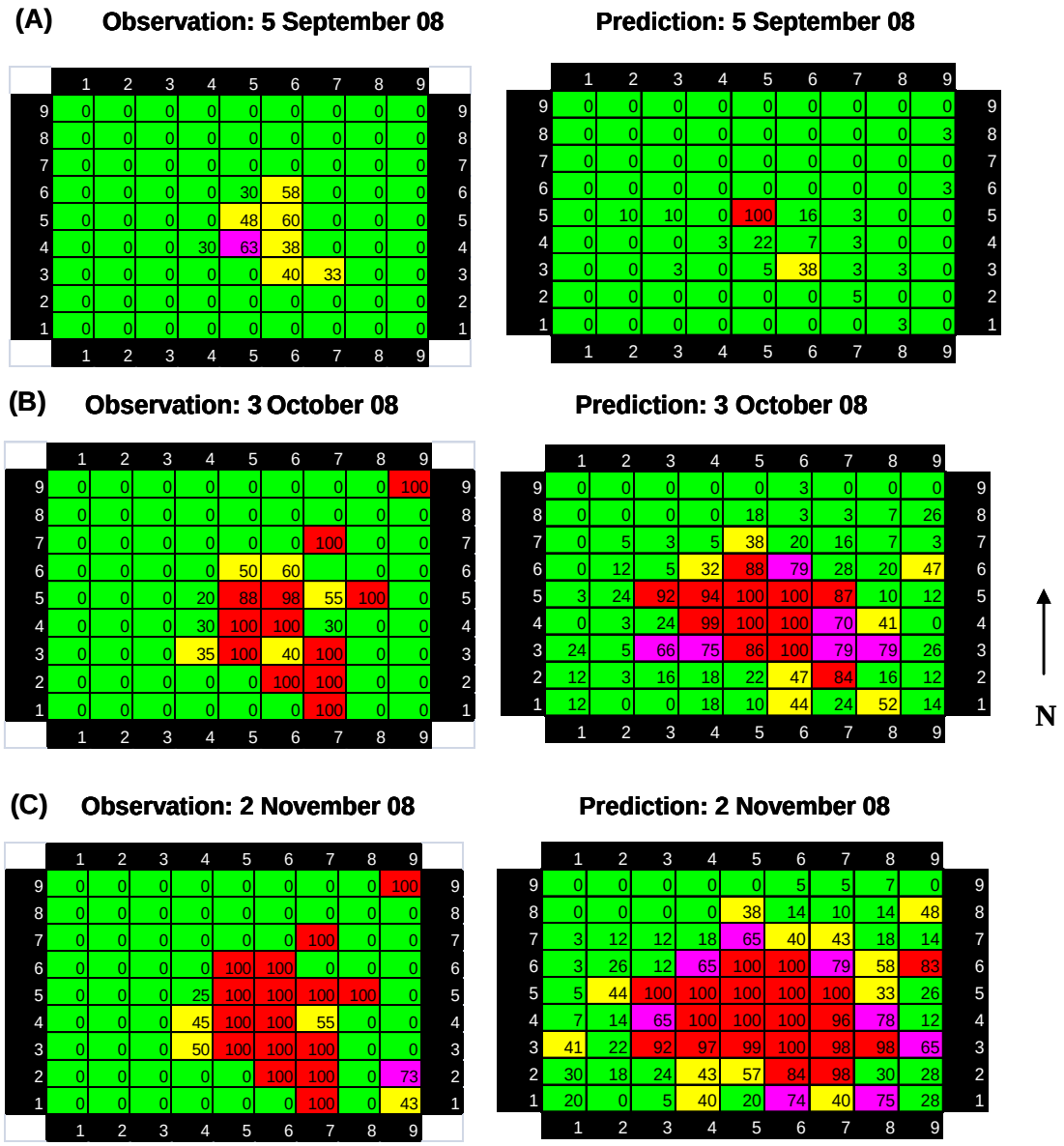

Figure 9 (A to C) Comparison of the observed (Obs) and modelled (Pre) mean plant infection (%) on 5 September, 3 October and 2 November 08, across (A) the whole plot, (B) the inner section of the plot and (C) the outer section of the plot. The bars indicate means and the lines indicate 99.9% confidence intervals.

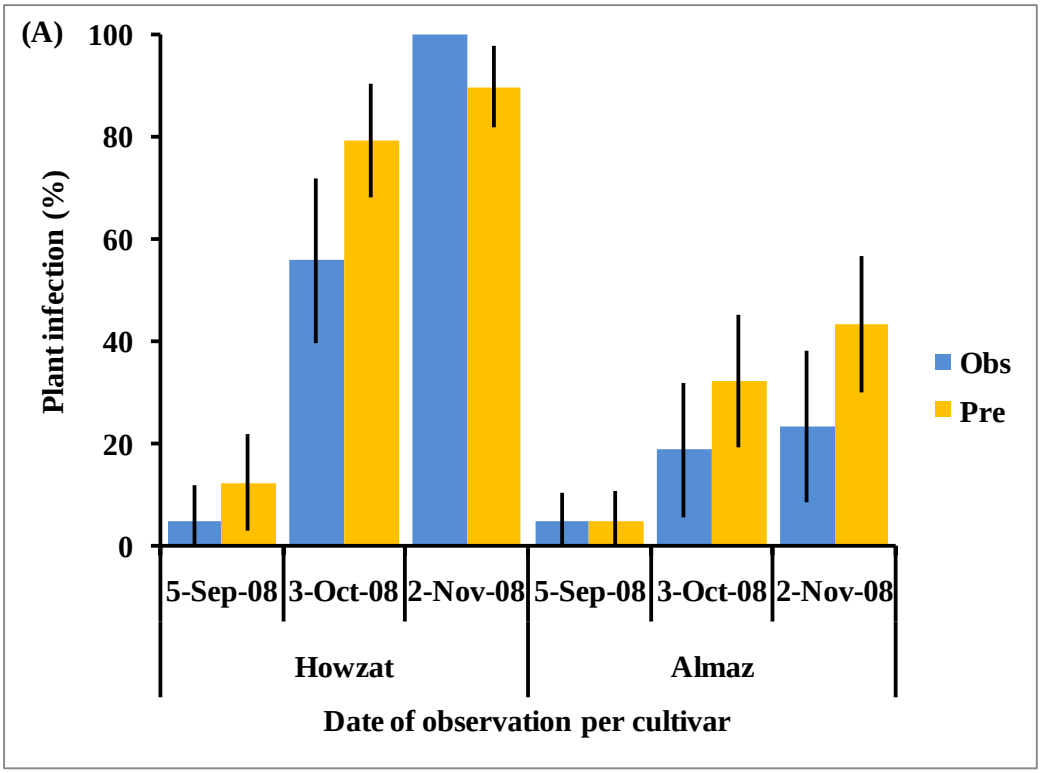

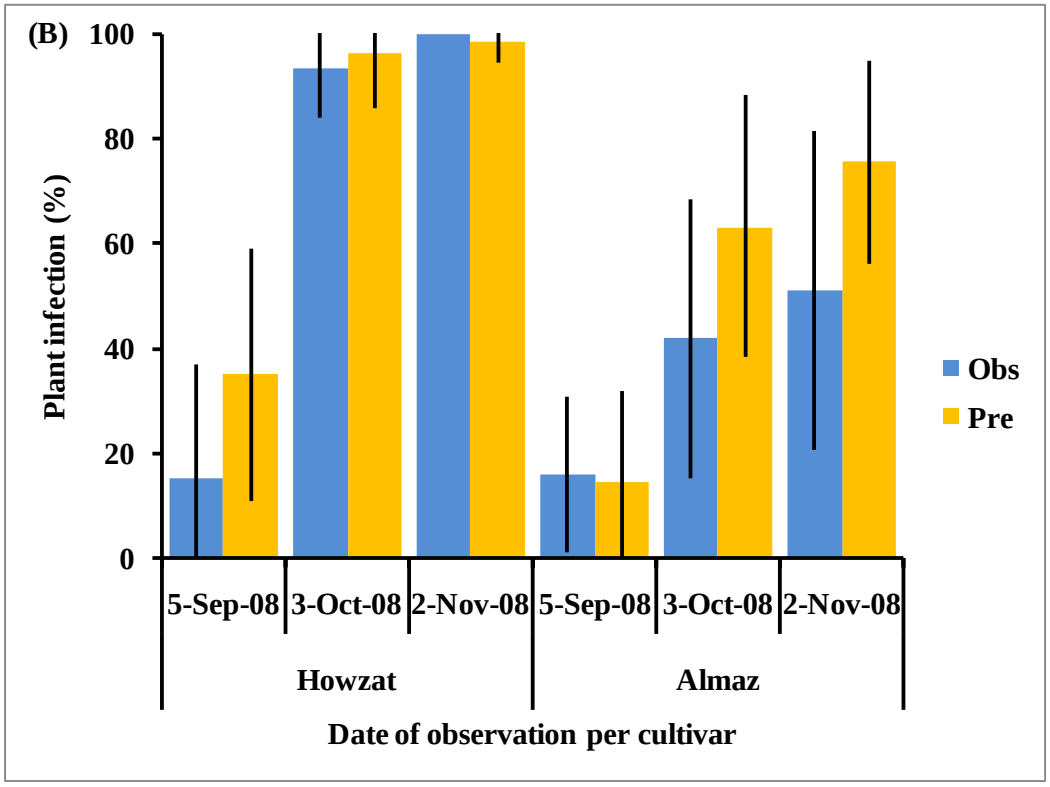
(B)
100
80
60
40
20
0
Plant infection (%)
Obs
Pre
5-Sep-08
3-Oct-08
2-Nov-08
5-Sep-08
3-Oct-08
2-Nov-08
Howzat
Almaz
Date of observation per cultivar

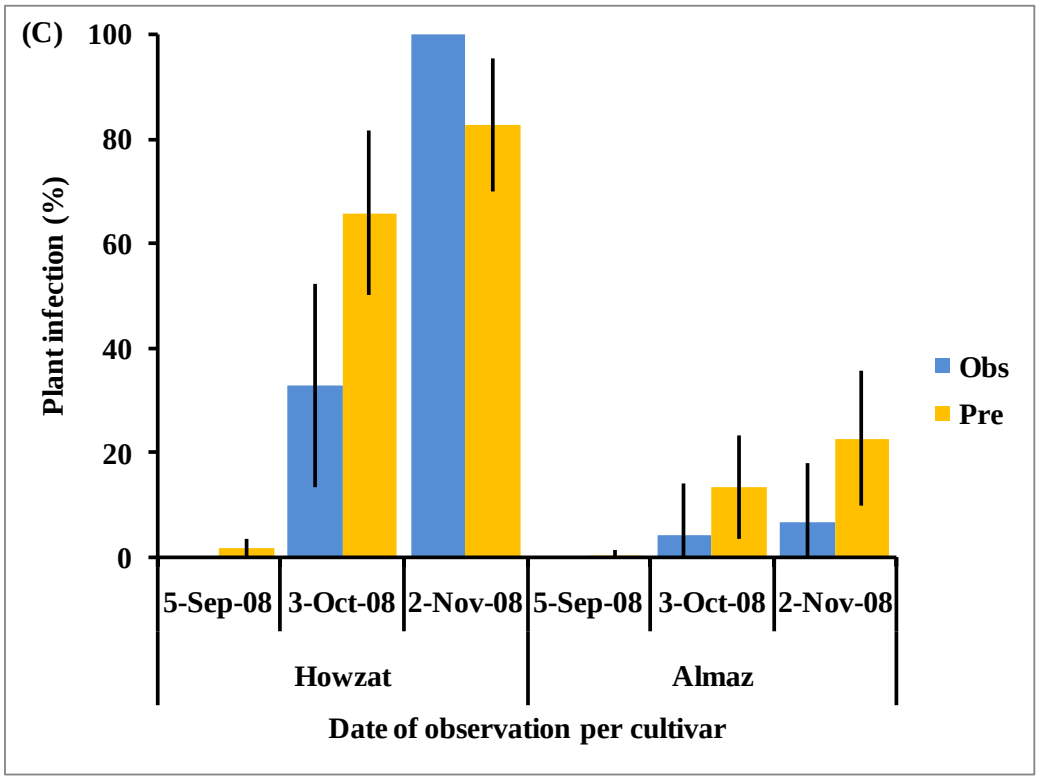
(C)
100
80
60
40
20
0
Plant infection (%)
Obs
Pre
5-Sep-08
3-Oct-08
2-Nov-08
5-Sep-08
3-Oct-08
2-Nov-08
Howzat
Almaz
Date of observation per cultivar

Figure 10 (A to C) Comparison of mean squared deviation (MSD) and its components; lack of correlation (LCS), weighted by the standard deviations (SDSD), and squared bias (SB), for the observed and predicted plant infection (%) on 5 September, 3 October and 2 November 2008 in cvs Howzat and Almaz. Performed over (A) the whole plot, (B) inner section of the plot and (C) outer section of the plot.

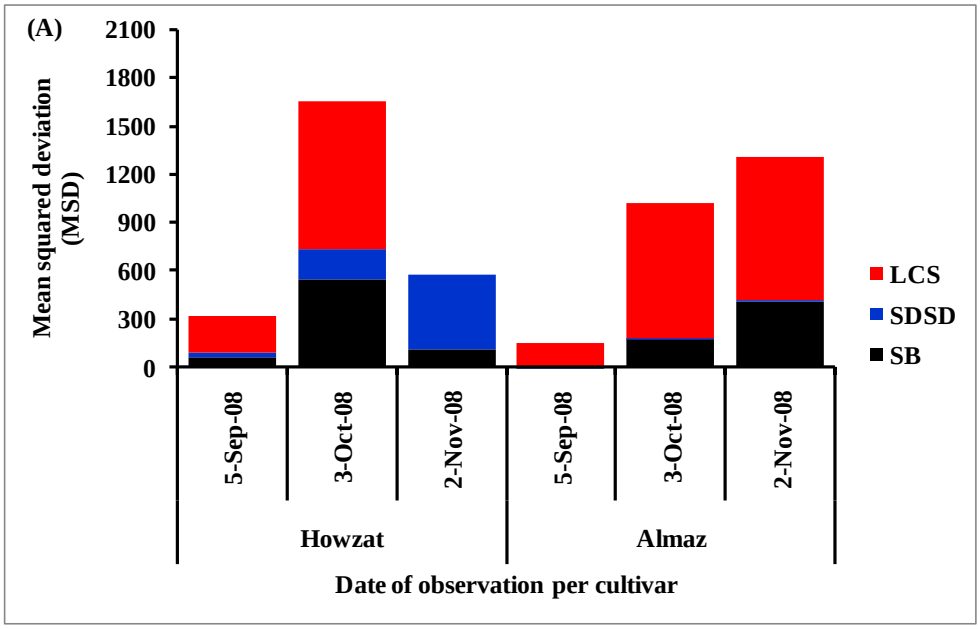

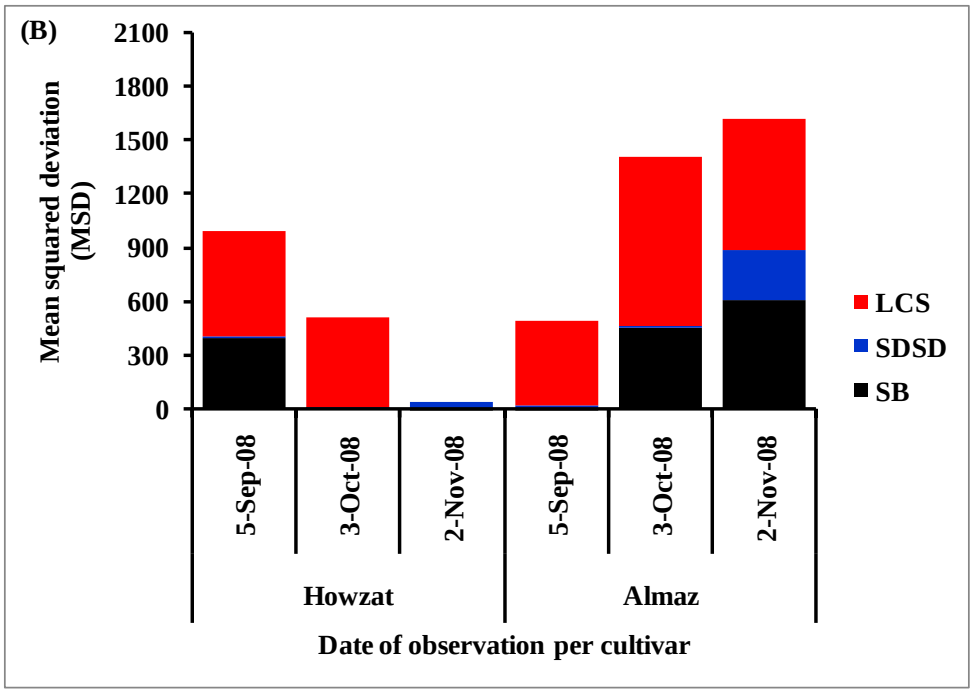

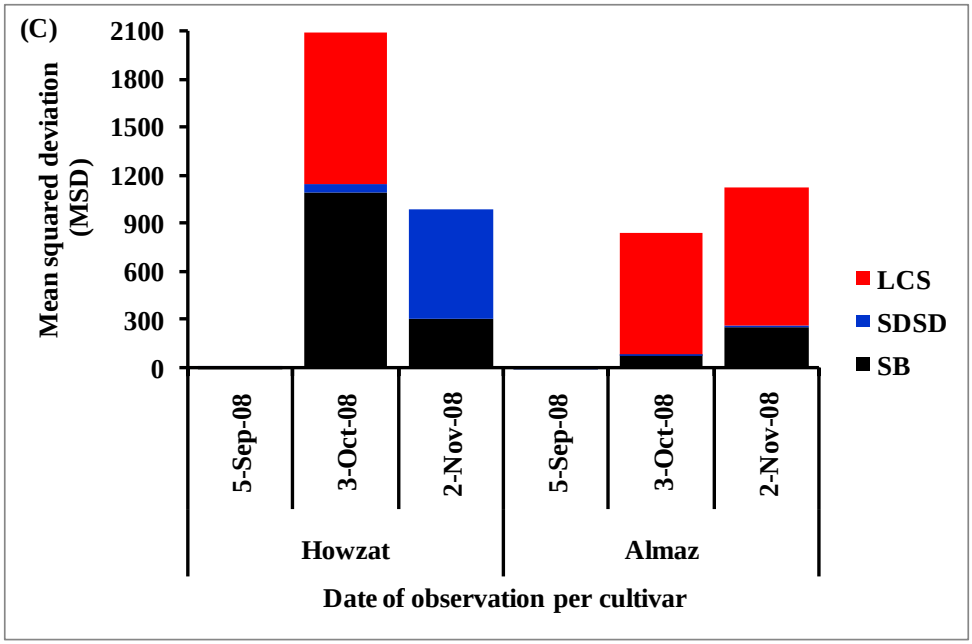
(C)
Mean squared deviation (MSD)
2100
1800
1500
1200
900
600
300
0
LCS
SDSD
SB
5-Sep-08
3-Oct-08
2-Nov-08
5-Sep-08
3-Oct-08
2-Nov-08
Howzat
Almaz
Date of observation per cultivar

Figure 11 Sensitivity analysis indicating parameters most affected by a change of ± 50 % from the original parameter value.